CARBON letters

Original Articles
Carbon Letters Vol. 26, 25-30 (2018)

Dispersion stability of polyelectrolyte-wrapped carbon black particles in a highly fluorinated solvent

Hyeon Ji Yoon, Jun Ho Choe, and Hyoung-Joon Jin*

WCSL (world Class Smart Lab) of Green Battery Lab., Department of Polymer Science and Engineering, Inha University, 100, Inha-ro, Nam-gu, Incheon 22212, South Korea

Article Info

Received 12 September 2017
Accepted 20 November 2017

***Corresponding Author**
E-mail: hjjin@inha.ac.kr

Open Access

DOI: http://dx.doi.org/10.5714/CL.2018.26.025

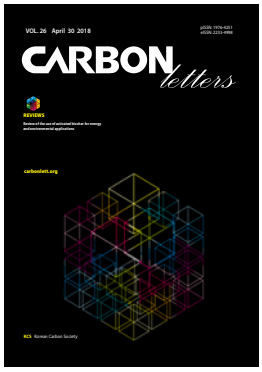

http://carbonlett.org

pISSN: 1976-4251
eISSN: 2233-4998

Abstract

The dielectric medium used in electrophoretic displays (EPDs) is required to be an environmentally friendly solvent with high density, low viscosity, and a large electric constant. Hydrofluoroether, a highly fluorinated solvent with eco-friendly characteristics, is regarded as a viable alternative medium for EPDs, owing to the similarity of its physical properties to those of the conventional EPD medium. Surface modification of particles is required, however, in order for it to disperse in the charged solvent. Also, positive/negative charges should be present on the particle surface to enable electrophoretic behavior. In this study, carbon black particles wrapped with positively charged nitrogen (N-CBs) were fabricated by a simple hydrothermal process using a poly(diallyldimethylammonium chloride) solution as a black coloring agent for the EPD. The dispersion behavior of N-CBs was investigated in various solvents.

Key words: Electrophoretic display; Fluorinated solvent; Carbon black; PDDA; Dispersion stability

1. Introduction

Electrophoretic displays (EPDs), which express text and images using movement of color-charged nanoparticles, have attracted attention owing to their low power consumption, flexibility, wide viewing angle, high reflectance, light weight, and potential for large-scale displays [1-3]. A pigment particle should fulfill the following three requirements in order to show electrophoretic behaviors: (1) distinguishable color, (2) conflicting charge, and (3) complete suspension in a dielectric medium. Halocarbon 0.8, which is an oligomer of chlorotrifluoroethylene, is widely used as the conventional dielectric medium for EPDs [4,5]. However, it presents an environmental hazard because of the chlorine atom present in each monomer unit [5]. Therefore, it is necessary to identify an environmentally friendly dispersion medium that is highly fluorinated (without chlorine) and to design charged particles with good dispersion stability in that solvent.

Pigment particles used in EPDs are usually synthesized through emulsion polymerization with a colored dye [6-9] or produced from nano-sized globular materials such as TiO_2 and carbon black (CB), which express white and black color, respectively [10-13]. CB has attracted attention owing to its good electrical and morphological properties. However, untreated CB nanoparticles are prone to assembling, owing to the small aggregate distance between the particles, strong van der Waals forces, and high surface tension of the nano-sized primary particles [14-16]. This grape-like morphology of CB causes difficulties in achieving uniform particle size, thereby hindering the performance of EPDs. It is essential to separate individual CB agglomerates to achieve a high-resolution EPD. Recently, several studies have sought to utilize CB nanoparticles as electrophoretic pigments via surface coating and grafting with polymers such as styrene, methyl methacrylate (MMA), and ethylene [17-20], as well as by functionalization of the particle surface [21-23]. However, these methods are

complex.

In this study, to substitute the halocarbon mixture, we used hydrofluoroether (HFE) (specifically, the HFE-7600 solvent, $C_5H_5G_6OC_3HF_6$) as a dielectric medium for an EPD, because of its low surface energy, low refractive index, chemical resistance, and ultraviolet (UV) stability, as well as the similarity of its physical properties to those of halocarbons, including low viscosity, high density, and high electric constant [24,25]. Nitrogen-wrapped carbon black particles (N-CBs) were prepared through a sonication/hydrothermal process with poly(diallyldimethylammonium chloride) (PDDA) solution. PDDA, which is a positively charged polyelectrolyte with linear chains, provided charged nitrogen on the surface of CB particles without color change [26-28]. Functionalizing nanocarbons with the PDDA polyelectrolyte enhanced their dispersion stability in various solvents. In particular, the obtained N-CBs showed improved dispersity in the HFE solvent.

2. Experimental

2.1 Preparation of N-CBs

CB powder (101 nm average particle diameter) was purchased from Powder Technology Inc. PDDA solution (20 wt% in H_2O) was purchased from Sigma-Aldrich. First, 100 mg of CB was added to 100 mL of deionized (DI) water and ultrasonicated for 1 h using an ultrasonic generator (Kyungill Ultrasonic Co., Korea). The power and frequency were fixed at 225 W and 20 kHz, respectively. Then, 200 mg of the PDDA solution was added to the CB solution. The PDDA-CB mixture was sonicated for 1 h and allowed to stand for 10 min. The mixture was subjected to a hydrothermal reaction process at 180 °C for 6 h. The resulting product was filtered and thoroughly washed with DI water and ethanol to remove any PDDA residue. The obtained sample (N-CBs) was redispersed in DI water and freeze-dried at -50 °C and 0.0045 mbar for 72 h. The resulting N-CBs were dried and stored in a vacuum oven at 30 °C. Sonication of CBs was carried out for 1 h and they were then freeze-dried under the same conditions as the N-CBs.

2.2 Characterization

The morphologies of CBs and N-CBs were examined using field-emission scanning electron microscopy (FE-SEM, S-4300SE, Hitachi, Japan) and field-emission transmission electron microscopy (FE-TEM, JEM2100F, JEOL, Japan). To investigate the carbon microstructure of samples, X-ray diffraction (XRD, Rigaku DMAX 2500) patterns were recorded using Cu-Kα radiation (wavelength λ = 0.154 nm) at 40 kV and 100 mA. Raman spectroscopy was carried out using a continuous-wave linearly polarized laser (wavelength 514.5 nm, excitation energy 2.41 eV, power 16 mW) with a 100× objective lens. The surface characteristics of the samples were investigated by X-ray photoelectron spectroscopy (XPS, PHI 5700 ESCA), using monochromatic Al Kα radiation with hv = 1486.6 eV. Fourier transform infrared (FT-IR) spectra of the samples were recorded using an infrared spectrometer (VERTEX 80V, Germany) in the spectral region of 4000–400 cm^{-1}. A zeta-potential analyzer (ELS-Z) was used to confirm the particle size distribution and zeta-potentials of N-CBs in HFE-7600.

2.3 Observation of N-CB dispersion behavior

The dried N-CBs (0.01 wt%) were ultrasonicated (power 200 W, frequency 20 kHz) for 10 min in various solvents: 20 g of water, ethanol (EtOH), methanol (MeOH), acetone, *N,N*-dimethylformamide (DMF), *N*-methyl-2-pyrrolidone (NMP), tetrahydrofuran (THF), xylene, hexane, and HFE-7600, respectively. The dispersion behaviors of N-CBs in various solvents were observed for 24 h. The dispersity of CBs and N-CBs were determined using a Turbiscan dispersion stability analyzer (Formulaction, France) for 48 h.

3. Results and discussion

3.1 Morphology and structural characteristics of N-CBs

Fig. 1(a) illustrates the process used for the preparation of N-CB particles. The N-CBs showed a split structure wrapped by PDDA polyelectrolyte after the sonication/hydrothermal process. The morphologies of CBs and N-CBs were investigated using FE-SEM and TEM. The two samples exhibited similar morphologies characterized by globular and aggregated nanometer-sized particles [Figs. 1(b)-(e)]. From the FE-SEM images, it was difficult to determine the degree of split of the nanoparticles, owing to powder sampling; further investigation was performed using TEM. The CBs were agglomerated, with particle sizes greater than 1 μm, as shown in Fig. 1(f). By contrast, after the sonication/hydrothermal processes, the N-CBs manifested split particles, with an average size of ~300 nm [Fig. 1(d)].

The microstructures of CBs and N-CBs were studied by XRD and Raman spectroscopy (Fig. 2). Notably, the XRD patterns of CBs and N-CBs showed two broad graphite (002) and (100) peaks around 24° and 44°, respectively, indicating that they have similar carbon ordering [Fig. 2(a)]. The Raman spectra of CBs and N-CBs showed D bands centered at 1348.7 and 1338.8 cm^{-1}, respectively, and G bands centered at 1572.9 and 1575.7 cm^{-1}, respectively [Fig. 2(b)]. The D bands were attributed to the breathing mode of A_{1g} symmetry of the sp^2 bonded carbon near the edges of rings, and the G bands were linked to the E_{2g} vibration modes of sp^2 carbon atoms. The ratios of the integrated intensities of the D and G bands (I_D/I_G) were ~0.94 and ~0.92 for CBs and N-CBs, respectively. The I_D/I_G ratios further indicated that the CBs and N-CBs were composed of few-nanometer-scale hexagonal carbon domains [29]. These results show that the sonication/hydrothermal process did not apparently affect the carbon microstructure of the N-CBs.

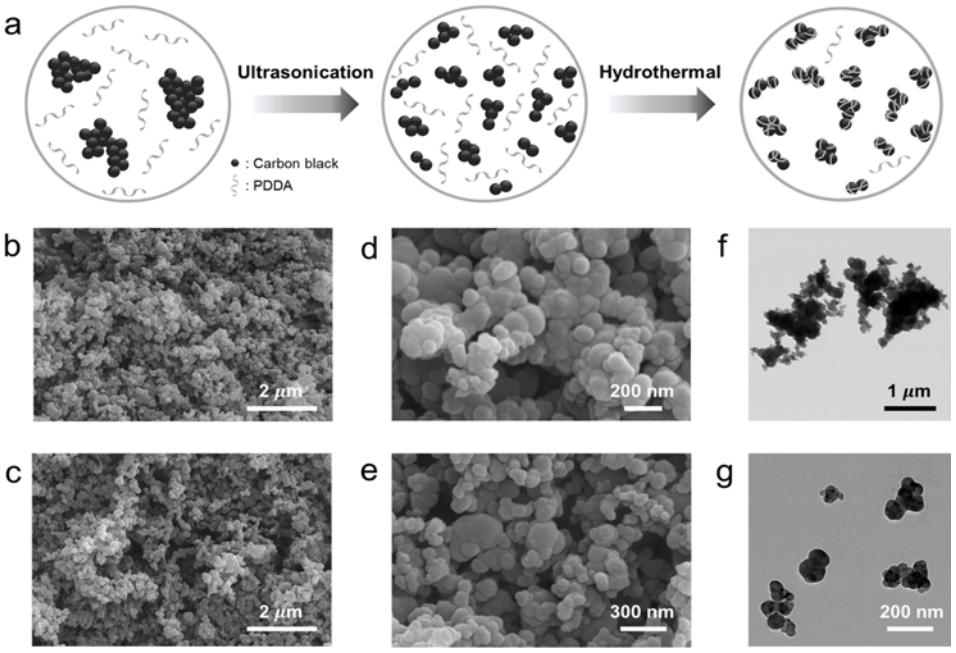

Fig. 1. (a) Schematic of the preparation of N-CBs. Morphological characteristics of the CBs and N-CBs. SEM images of the (b-c) CBs and (d-e) N-CBs under different magnifications. FE-TEM images of the (f) CNs and (g) N-CBs.

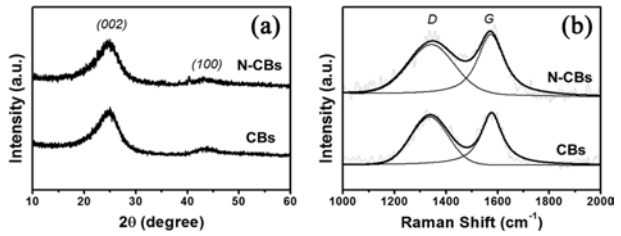

Fig. 2. Microstructures of N-CBs and CBs. (a) X-ray diffraction patterns and (b) Raman spectra of N-CBs and CBs.

3.2 Chemical structure of N-CBs

XPS experiments were performed to investigate the surface chemical properties of CBs and N-CBs. As shown in Fig. 3(a), several peaks were observed in the C 1*s* spectra of CBs, centered at 284.3 eV (sp^2 C=C), 284.8 eV (sp^3 C-C), 286.0 eV (C-O), and 289.9 eV (O=C-O bonds). After the hydrothermal process, similar peaks from sp^2 C=C, sp^3 C-C, C-O, and O=C-O bonds, centered at 284.3, 284.8, 286.2, and 289.8 eV, respectively, were observed in the C 1*s* spectra of N-CBs [Fig. 3(a)]. In the O 1*s* spectra of CBs and N-CBs, C=O bonding centered at 531.2 eV and C-O bonding centered at 533.0 eV were observed [Fig. 3(b)]. The nitrogen signal in the N-CB spectra came from the PDDA polyelectrolyte. The N 1*s* spectra of N-CBs exhibited a distinct peak centered at 402.6 eV, indicating charged nitrogen (N^+). Another peak, appearing at 397.0 eV, could be attributed to the cyano group (C=N) [Fig. 3(c)]. Positively charged nitrogen groups on the N-CBs can improve the dispersion stability in various solvents owing to repulsive interactions, preventing the reunion of nanoparticles [27]. The C/O and C/N ratios of N-CBs were 5.07 and 35.96, respectively, indicating that numerous heteroatoms were present on the surfaces of N-CBs.

Fig. 3(d) shows the FT-IR spectra of CBs and N-CBs. Concordant peaks were observed at 1,400 and 1,635 cm^{-1}, which could be interpreted as C-O-C bonding and C=O stretching, respectively. Peaks corresponding to C-H stretching and the methyl ($-CH_3$) bond appeared in all samples, centered at 2,923 and 2,860 cm^{-1}. In contrast, the peak at 1,460 cm^{-1}, related to the C-N bond, was found only in the spectrum of the N-CBs. Absorption peaks between 1,000 and 1,200 cm^{-1} were also observed in the N-CBs, owing to the presence of small aliphatic amines on the nanoparticle surfaces. These results prove that the nitrogen functionalities in N-CBs were successfully introduced from the PDDA polyelectrolyte by the hydrothermal process, in agreement with the XPS analysis.

3.3. Dispersion stability of N-CBs

To predict dispersion behavior, the CBs and N-CBs were dispersed in various solvents, categorized as polar protic (water, EtOH, and MeOH), polar aprotic (acetone, DMF, NMP, and THF), and non-polar (xylene, toluene, and hexane), for 24 h [Fig. 4(a)]. We discussed using a Hansen solubility parameter that included δ_d, δ_p, and δ_h, indicating the dispersion cohesion, polarity cohesion, and hydrogen bonding cohesion parameters, respectively [30-33]. Table 1 lists the parameters and surface energy values for each solvent. The N-CBs did not disperse in xylene, toluene, or hexane, which are non-polar solvents with hydrophobic properties ($\delta_p+\delta_h < 10$ $MPa^{1/2}$), suggesting that the dispersion stability of N-CBs is affected by the polar characteristics of the dispersion medium. A homogeneous colloidal suspension of N-CBs was obtained in the protic polar solvents (water, ethanol, and methanol), with high $\delta_p+\delta_h$ values

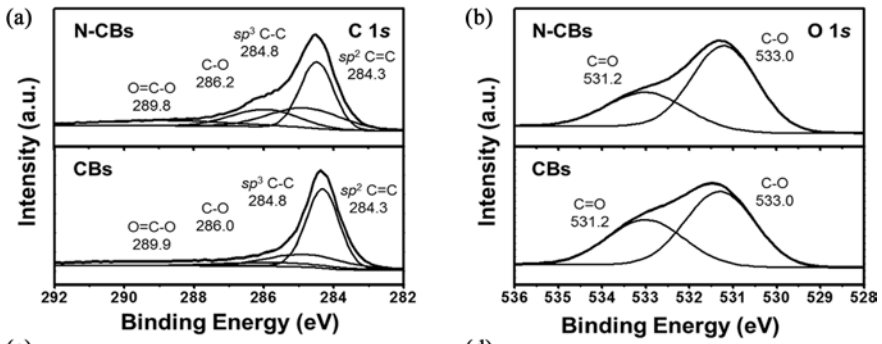

	C 1*s*	O 1*s*	N 1*s*
N-CBs	81.64	16.09	2.27
CBs	94.81	4.29	-

Fig. 3. Surface chemical properties of N-CBs and CBs. XPS analysis: (a) C 1*s* and (b) O 1*s* spectra of N-CBs and CBs. (c) N 1*s* spectra of N-CBs. (d) FT-IR spectra of N-CBs and CBs.

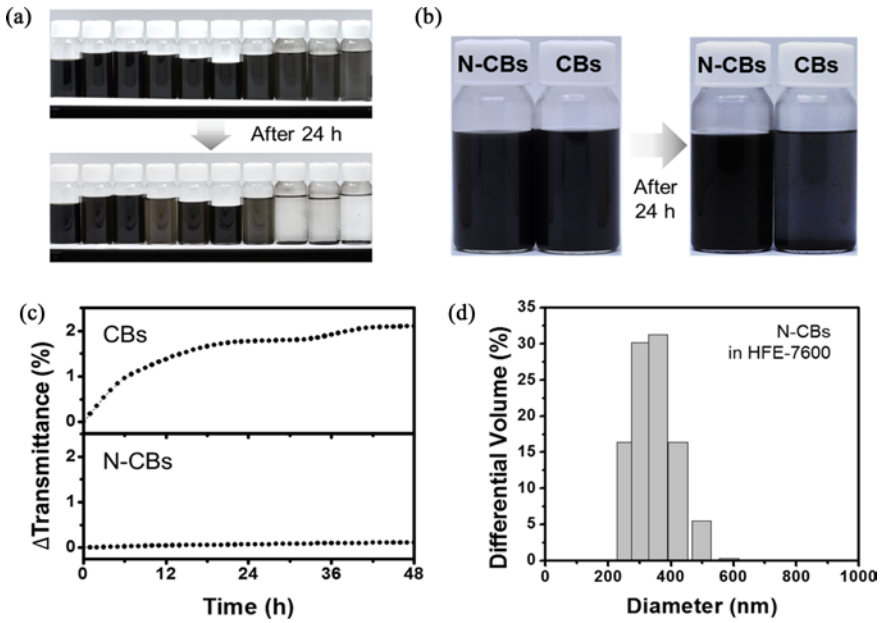

Fig. 4. (a) Dispersion images of 0.01 wt% N-CBs in various solvents after 24 h. (form left : Water, Ethanol, Methanol, Acetone, DMF, NMP, THF, Xylene, Toluene, Hexane) (b) Dispersion images of CBs and N-CBs in HFE-7600. (c) Turbiscan data of CBs and N-CBs in HFE-7600. (d) Particle size distribution data for N-CBs in HFE-7600.

in a range of 22.1–58.3 $MPa^{1/2}$. In the case of aprotic solvents, the dispersion behavior of N-CBs differed depending on the characteristics of the particular solvent. A solvent with a large dipole moment makes it easier to solvate charged particles, owing to the dominant interactions between the dipole and the solute. For example, NMP and DMF, which have high dipole moments (4.09 D and 3.82 D, respectively) and surface tensions ($\gamma \geq 37.10$ mJ m^{-2}) and a $\delta_p+\delta_h$ value greater than 20 $MPa^{1/2}$ (i.e., hydrophilic properties), showed good dispersity of N-CBs. HFE-7600 has a high electrical dipole moment (3.88 D, obtained by density functional theory calculations) due to its asymmetric molecular structure and exhibited similar dispersion stability to NMP [Fig. 4(b)] [34].

Table 1. Dispersion stability of N-CBs with Hansen solubility parameters and surface tension.

Solvent	δ_d	δ_p	δ_h	$\delta_p+\delta_h$	g	N-CBs
Water	15.5	16	42.3	58.3	72.8	++++
Ethanol	15.8	8.8	19.4	28.2	22.1	+++
Methanol	15.1	12.3	22.3	34.6	22.7	++++
Acetone	15.5	10.4	7.0	17.4	25.2	+
DMF	17.4	13.7	11.3	25.0	37.1	+++
NMP	18.0	12.3	7.2	19.5	40.8	++++
THF	16.8	5.7	8.0	13.7	26.4	+
Xylene	17.6	1.0	3.1	4.1	28.9	-
Toluene	18.0	1.4	2.0	3.4	28.4	-
n-Hexane	14.9	0	0	0	18.4	-

The stabilities of CBs and N-CBs dispersed in HFE-7600 were investigated using multiple light scattering [Fig. 4(c)]. The time *versus* transmittance variation was used to provide quantitative dispersity measurements for the samples [32]. In HFE-7600, the N-CBs showed little transmittance variation after 48 h. On the contrary, the transmittance variation for the CBs increased rapidly to approximately 2.10% in the same medium. These results confirmed that the N-CBs had good dispersion stability in the HFE-7600 solvent.

Fig. 4(d) shows the particle size distribution of N-CBs dispersed in HFE-7600, from 250 to 600 nm. Considering that the average particle diameter of CB is approximately 101 nm, this indicates that two or three nanoparticles were aggregated. On the other hand, the average particle size of CBs was ~24,131 nm in the same solvent, consistent with the TEM images [Figs. 1(f)-(g)]. Additionally, the zeta-potentials of the N-CBs were 35.7 and 32.5 mV in water and HFE-7600, respectively. In HFE-7600, the value of N-CBs was higher than that of CBs, indicating that charged nitrogen groups were successfully introduced on the surfaces of N-CBs.

4. Conclusion

In summary, we prepared black particles for EPD systems from carbon black by wrapping them with PDDA polyelectrolyte. The N-CBs maintained their intrinsic carbon microstructures after sonication/hydrothermal reaction, and successfully split into small particles with an average diameter of about 344 nm. The surface chemical properties were confirmed by XPS and FT-IR analyses. The charged nitrogen, N^+, was confirmed to be present on the surfaces of the N-CBs. The dispersion stability of N-CBs in various solvents was compared, using multiple light scattering and zeta-potential analyses. The N-CBs formed a stable colloidal suspension in solvents with large dipole moments, hydrophilic properties, and high surface tensions. In particular, N-CBs showed excellent dispersion behaviors in HFE-7600, indicating its potential as an environmentally friendly fluorinated solvent for EPDs.

Acknowledgments

This study was supported by a grant (#10067681) from the Fundamental R&D Program for Core Technology of Materials funded by the Korean Ministry of Trade, Industry and Energy. This work was also supported by the Civil-Military Technology Cooperation Program (Project No. 17-CM-DP-22) funded by the Defense Acquisition Program Administration, Republic of Korea.

References

[1] Comiskey B, Albert JD, Yoshizawa H, Jacobson J, An electrophoretic ink for all-printed reflective electronic displays. Nature, 394, 253 (1998). doi: 10.1038/28349.

[2] Xiao L, Zheng X, Zhao T, Sun L, Liu F, Gao G, Dong A, Controllable immobilization of polyacrylamide onto glass slide: synthesis and characterization. Colloid Polym Sci, 291, 2359 (2013). Doi: 10.1007/s00396-013-2981-2.

[3] Werts MPL, Badila M, Brochon C, Hébraud A, Hadziioannou G, Titanium dioxide−polymer core–shell particles dispersions as electronic inks for electrophoretic displays. Chem Mater, 20, 1292 (2008). doi: 10.1021/cm071197y.

[4] Song JK, Choi HJ, Chin I, Preparation and properties of electrophoretic microcapsules for electronic paper. J Microencapsul, 24, 11 (2007). doi: 10.1080/02652040601058384.

[5] Bolaji BO, Huan Z, Ozone depletion and global warming: Case for the use of natural refrigerant –a review. Renew Sust Energ Rev, 18, 49 (2013). doi: 10.1016/j.rser.2012.10.008.

[6] Belsey KE, Topping C, Farrand LD, Holder SJ, Inhibiting the thermal gelation of copolymer stabilized nonaqueous dispersions and the synthesis of full color PMMA particles. Langmuir, 32, 2556 (2016). doi: 10.1021/acs.langmuir.6b00063.

[7] Fang Y, Wang S, Xiao Y, Li X, Preparation and properties of red inorganic hollow nanospheres for electrophoretic display. Appl Surf Sci, 317, 319 (2104). doi: 10.1016/j.apsusc.2014.08.121.

[8] Fang K, Ren B, A facile method for preparing colored nanospheres

of poly(styrene-co-acrylic acid). Dyes Pigment, 100, 50 (2014). doi: 10.1016/j.dyepig.2013.07.021.

[9] Qi D, Cao Z, Ziener U, Recent advances in the preparation of hybrid nanoparticles in miniemulsions. Adv Colloid Interface Sci, 211, 47 (2014). doi: 10.1016/j.cis.2014.06.001.

[10] Park KJ, Lee KU, Kim MH, Kwon OJ, Kim JJ, Preparation of PS/TiO_2 as a white pigment for electrophoretic displays. Curr Appl Phys, 13, 1231 (2013). doi: 10.1016/j.cap.2013.03.020.

[11] Kim KS, Lee JY, Park BJ, Sung JH, Chin I, Choi HJ, Lee JH, Synthesis and characteristics of microcapsules containing electrophoretic particle suspensions. Colloid Polym Sci, 284, 813 (2006). doi: 10.1007/s00396-006-1465-z.

[12] Maiti J, Basfar AA, Encapsulation of carbon black by surfactant free emulsion polymerization process. Macromol Res, 25, 120 (2017). doi: 10.1007/s13233-017-5023-y.

[13] Tan T, Wang S, Bian S, Li X, An Y, Liu Z, Novel synthesis and electrophoretic response of low density TiO–TiO_2–carbon black composite. Appl Surf Sci, 256, 6932 (2010). doi: 10.1016/j.apsusc.2010.04.061.

[14] Lee KU, Park KJ, Kwon OJ, Kim JJ, Carbon sphere as a black pigment for an electronic paper. Curr Appl Phys, 13, 419 (2013). doi: 10.1016/j.cap.2012.09.003.

[15] Szeluga U, Kumanek B, Trzebicka B, Synergy in hybrid polymer/nanocarbon composites. A review. Compos Pt A, 73, 204 (2015). doi: 10.1016/j.compositesa.2015.02.021.

[16] Lahaye J, Ehrburger-Dolle F, Mechanisms of carbon black formation. Correlation with the morphology of aggregates. Carbon, 32, 1319 (1994). doi: 10.1016/0008-6223(94)90118-X.

[17] Fu S, Zhang L, Tian A, Xu Y, Du C, Xu C, Preparation of a novel colorant with branched poly(styrene-alt-maleic anhydride) for textile printing. Ind Eng Chem Res, 53, 10007 (2014). doi: 10.1021/ie500865e.

[18] Ridaoui H, Jada A, Vidal L, Donnet JB, Effect of cationic surfactant and block copolymer on carbon black particle surface charge and size. Colloid Surf A-Physicochem Eng Asp, 278, 149 (2006). doi: 10.1016/j.colsurfa.2005.12.013.

[19] Chou IC, Chen SI, Chiu WY, Surfactant-free dispersion polymerization as an efficient synthesis route to a successful encapsulation of nanoparticles. RSC Adv, 4, 47436 (2014). doi: 10.1039/c4ra07475k.

[20] Kim M, Park KJ, Lee KU, Kim MJ, Kim WS, Kwon OJ, Kim JJ, Preparation of black pigment with the Couette–Taylor vortex for electrophoretic displays. Chem Eng Sci, 119, 245 (2014). doi: 10.1016/j.ces.2014.08.036.

[21] Kim JY, Oh JY, Suh KS, Voltage switchable surface-modified carbon black nanoparticles for dual-particle electrophoretic displays. Carbon, 66, 361 (2014). doi: 10.1016/j.carbon.2013.09.011.

[22] Gacek MM, Berg JC, The role of acid–base effects on particle charging in apolar media. Adv Colloid Interface Sci, 220, 108 (2015). doi: 10.1016/j.cis.2015.03.004.

[23] Yang F, Xin L, Uzunoglu A, Qiu Y, Stanciu L, Ilavsky J, Li W, Xie J, Investigation of the interaction between nafion ionomer and surface functionalized carbon black using both ultrasmall angle x-ray scattering and cryo-TEM. ACS Appl Mater Interfaces, 9, 6530 (2017). doi: 10.1021/acsami.6b12949.

[24] Tsai WT, Environmental risk assessment of hydrofluoroethers (HFEs). J Hazard Mater, A119, 69 (2005). doi: 10.1016/j.jhazmat.2004.12.018.

[25] Sekiya A, Misaki S, The potential of hydrofluoroethers to replace CFCs, HCFCs and PFCs. J Fluor Chem, 101, 215 (2000). doi: 10.1016/S0022-1139(99)00162-1.

[26] Kim H, Jo SH, Jee JH, Han W, Kim Y, Park HH, Jin HJ, Yoo B, Lee JK, Fluorous-inorganic hybrid dielectric materials for solution-processed electronic devices. New J Chem, 39, 836 (2015). doi: 10.1039/c4nj01435a.

[27] Xue YH, Zhou WJ, Zhang L, Li M, Chan SH, Poly (diallyldimethylammonium chloride)-functionalized reduced graphene oxide supported palladium nanoparticles for enhanced methanol oxidation. RSC Adv, 5, 32983 (2015). doi: 10.1039/C4RA16694A.

[28] Yang Y, Hao Y, Yuan J, Niu L, Xia F, In situ co-deposition of nickel hexacyanoferrate nanocubes on the reduced graphene oxides for supercapacitors. Carbon, 84, 174 (2015). doi: 10.1016/j.carbon.2014.12.005.

[29] Cho SY, Yun YS, Lee S, Jang D, Park KY, Kim JK, Kim BH, Kang K, Kaplan DL, Jin HJ, Carbonization of a stable β-sheet-rich silk protein into a pseudographitic pyroprotein. Nat Commun, 6, 7145 (2015). doi: 10.1038/ncomms8145.

[30] Hansen CM, Hansen solubility parameters: a user's handbook; 2nd edition, CRC Press: Hoboken (2007).

[31] Park S, An J, Jung I, Riner RD, An SJ, Li X, Velamakanni A, Ruoff RS, Colloidal suspensions of highly reduced graphene oxide in a wide variety of organic solvents. Nano Lett, 9, 1593 (2009). doi: 10.1021/nl803798y.

[32] Song MY, Yun YS, Kim NR, Jin HJ, Dispersion stability of chemically reduced graphene oxide nanoribbons in organic solvents. RSC Adv, 6, 19389 (2016). doi: 10.1039/c5ra23801c.

[33] Kim DH, Yun YS, Jin HJ, Difference of dispersion behavior between graphene oxide and oxidized carbon nanotubes in polar organic solvents. Curr Appl Phys, 12, 637 (2012). doi: 10.1016/j.cap.2011.09.015.

[34] Abe H, Imai Y, Tokunaga N, Yamashita Y, Sasaki Y, Highly efficient electrohydrodynamic pumping: molecular isomer effect of dielectric liquids, and surface states of electrodes. ACS Appl Mater Interfaces, 7, 24492 (2015). doi: 10.1021/acsami.5b05778.